Raman spectroscopy and x-ray diffraction measurements on C_{60} compressed in a diamond anvil cell

Y. Li, J. H. Rhee, D. Singh, and S. C. Sharma*
Department of Physics, Box 19059, University of Texas at Arlington, Arlington, Texas 76019, USA
(Received 3 September 2002; revised manuscript received 21 February 2003; published 28 July 2003)

Using Raman spectroscopy, we present evidence for pressure-induced phase transitions of C_{60} compressed up to 31.1 GPa in a diamond anvil cell at room temperature. No significant change is observed in the Raman spectra upon release of pressure from 31.1 GPa down to almost ambient; the material retains its high pressure phase present at 31.1 GPa. By using x-ray diffraction measurements with a 300-μm-diameter collimated x-ray beam, we identify the high-pressure (31.1 GPa) structure of the material. It is found to be a mixture of the body-centered orthorhombic (*Immm*), rhombohedral ($R\bar{3}m$), and an unidentified phase.

DOI: 10.1103/PhysRevB.68.024106 PACS number(s): 61.48.+c, 62.50.+p, 78.30.−j, 61.10.−i

I. INTRODUCTION

The properties of C_{60} fullerenes under high pressures and different temperatures continue to be of significant interest.[1–6] The pressure-temperature (P-T) phase diagram of C_{60} has been studied, in the majority of the published works, using quenched samples that are prepared by high-pressure high-temperature (HPHT) treatments (usually, $2 < P \leqslant 8$ GPa and $300 < T \leqslant 1920$ K) and subsequently compressed under high pressures.[1–4,7–15] It is known that several kinds of polymerized phases of C_{60} can be realized in thus-prepared and treated samples.[6,11] In spite of a significant level of activity, the phase diagram of C_{60} continues to be the subject of discussion. At room temperature, a phase transition was reported by Chandrabhas *et al.*,[15] who observed a significant decrease in the Raman frequency of the $A_g(2)$ mode of C_{60} at 0.35 GPa. Further, infrared (IR) spectroscopy studies by Yamawaki *et al.*[16] showed appearance of new absorption bands and marked reduction in the intensity of the original bands at about 4 GPa due to pressure (hydrostatic) induced polymerization of C_{60}. Yoo and Nellis reported a phase transformation at room temperature from weakly interacting C_{60} molecules to strongly interacting C_{60} agglomerates or networks under high static pressures; the transition being reversible between 15 and 25 GPa and irreversible above 27 GPa.[17] These authors further observed that all of the vibrational modes shifted linearly with pressure up to about 10 GPa and deviated from linearity with the appearance of a ''knee'' between 10 and 15 GPa. Nishikawa *et al.* suggested a phase transition at around 0.6 GPa.[18] Blank *et al.*[19] have presented evidence for several structural phase transitions at 0.3, 2.3, 6, and 18 GPa under controlled shear deformations. The early work on the polymerized phases of C_{60} is summarized in excellent works by Eklund and Rao,[6] Dresselhaus *et al.*,[20] Kadish and Ruoff,[21] and Sundqvist.[22] The pressure-induced phases of quenched C_{60} have been further studied in more details in several recent investigations.[1,2,4]

Most recently Talyzin *et al.* have presented results of a detailed study on the pressure-induced polymerization of C_{60} at high temperatures.[1] These authors have studied a diagonal section of the P-T diagram in HPHT samples starting from room temperature and 5.5 GPa, heating the sample up to 780 K and 1.5 GPa, followed by cooling down to room temperature and 7.5 GPa. According to this study, the polymerization proceeds during the heating cycle, from monomeric C_{60} to dimeric-one-dimensional (1D) polymer, orthorhombic (O) to 2D polymer, consisting of a tetragonal (T) and rhombohedral (R) phases, experimental evidence for phase-T as a stable high-pressure phase had been presented in an earlier study by Davydov *et al.*[23] Using different paths of the HPHT treatment, Davydov *et al.*[23] had obtained phase-T as a product of phase conversions of a monomeric fcc and two polymerized phases of C_{60}, including phase-R at 2.2 GPa and 873 K. Following Davydov *et al.*,[23] Talyzin *et al.*[1] report that a preferential pathway to prepare the tetragonal phase seems to be a high-temperature treatment followed by pressure increase, and for the rhombohedral phase a pressure treatment followed by high temperature. In a quenched sample, Talyzin *et al.* observe a mixture of the orthorhombic and tetragonal phases with a small addition of the rhombohedral phase. In another recent study, Meletov *et al.*[2] have investigated the effect of pressure on 2D tetragonal C_{60} polymer sample that was prepared by pressurizing pristine C_{60} within 2.3–2.5 GPa at about 820 K. These authors observe a gradual phase transformation between 19 and 21 GPa. Based on the Raman scattering data, they believe that the C_{60} cage is retained and the high-pressure phase of their sample is related to a 3D polymerized phase. This is in good agreement with Okada *et al.*[24] who had previously presented evidence based on the density functional theory for a stable 3D polymerized C_{60} structure under uniaxial pressures of about 20 GPa. Adam and Page[25] have used an approximate first-principles method together with a bond-polarizability model to calculate theoretical Raman spectra for the orthorhombic (O), tetragonal (T), and rhombohedral (R) phases of pressure-polymerized C_{60}. Burgos *et al.*[26] have studied possible phases of 3D C_{60}-based fullerites using semiempirical potentials and *ab initio* density-functional methods. They present theoretical evidence for three closely related structures: two body-centered orthorhombic and one body-centered cubic; 3D polymers with semiconducting properties. Chernozatonskii *et al.*[27] also present analysis of x-ray diffraction patterns on HPHT quenched samples (13 GPa and 670–820 K) supporting the formation of a 3D polymerized phase. Davydov *et al.*[4] and Marques *et al.*[28] have presented evidence for pressure-polymerized phases of C_{60}. Blank *et al.*[29] have pre-

sented collection and analysis of data on high-pressure polymerized phases of C_{60} with a pressure-temperature phase diagram up to 20 GPa and 2300 K. Obviously, properties of C_{60}-based materials, and in particular of its polymerized phases, continue to be the subject of significant research activity. However, as stated above, a large number of the investigations have focused on samples prepared by the HPHT treatments and subsequently subjected to high pressures. Since, the eventual structure of the material may depend on the synthesis route employed, it is of interest to investigate effects of pressure on samples synthesized by techniques that do not rely solely on the HPHT treatment.

In the present work, we have advanced our preliminary work, reported elsewhere,[30–32] on the effects of pressure on the structure of C_{60} in samples that are not prepared by the HPHT treatment. Using high-resolution Raman spectroscopy, we present evidence for structural phase transitions and observe that the material retains its structure that existed under 31.1 GPa at room temperature. Additionally, by using x-ray diffraction analysis with a 300-μm-diameter collimated x-ray beam, we identify the high-pressure (31.1 GPa) structure of C_{60}, consisting of a mixture of body-centered orthorhombic, rhombohedral, and an unidentified phase. Interesting results of our work on the non-HPHT samples can be summarized as follows: (i) similar to the earlier results on the HPHT samples, we too observe pressure-induced phase transitions, (ii) we characterize the crystal structure of the high-pressure (31.1 GPa) phase as a mixture of the body-centered orthorhombic, rhombohedral, and an unidentified phase, and (iii) at variance with the results on the HPHT samples, we do not observe the so-called hard and superhard phases in our sample after it has been subjected to four different sequences of pressures (described below) between ambient and 31.1 GPa.

The outline of the remainder of the manuscript is as follows: Section II provides a brief summary of the experimental details, Sec. III presents the main results and their discussion, and Sec. IV presents the conclusions.

II. EXPERIMENTAL DETAILS

The C_{60} powder of 99.9% purity and containing 1–10-μm particles, obtained from MER, was used in this work.[33] High-resolution Raman spectra were measured by using a 1.25-m, f/11 monochromator, 1200- and 2400-g/mm ion-etched blazed holographic diffraction gratings, liquid-nitrogen-cooled charge-coupled device (CCD) camera, Super-Notch-Plus filter, argon-ion laser operating at 514.5 nm and at $\leqslant$100 mW (assuming a Gaussian beam profile for the 2.4×10^{-3}-m-diameter laser beam, the spot size on the sample is estimated to be about $\leqslant10$ μm), and SpectraMax for Windows software. The C_{60} powder was loaded in a diamond anvil cell (DAC) containing pre-indented stainless steel gasket with a 200-μm hole. We present data from two sets of experiments that were conducted: (i) without using a pressure transmitting medium in the DAC (uniaxial pressure), and (ii) by using a mixture of methanol:ethanol:water (16:3:1) as the pressure transmitting medium in the DAC (nearly hydrostatic pressure). This particular pressure transmitting medium has been characterized with a range of nearly hydrostatic behavior up to about 10 GPa,[34] as well as up to about 20 GPa with a freezing pressure of 14.5 GPa at room temperature.[35] In any event, the data measured with the use of this transmitting medium in the DAC are under nearly hydrostatic pressures at least up to about 10 GPa. Because of the mechanical mechanism by which pressure is increased by tightening, one by one, four screws on the DAC; it is possible that the sample experiences shear deformation. Applied pressures were calculated by measuring pressure-induced shifts in the Ruby fluorescence peaks. The measured Raman spectra were analyzed for the central frequency of the bands and their full width at half maximum (FWHM) by nonlinear least-squares technique by using Gaussian functions. The performance of the Raman spectrometer and the accuracy of the data analysis techniques were thoroughly tested by repeated measurements of the well-known Raman bands in several materials, i.e., 1332-cm^{-1} line of diamond, 521-cm^{-1} line of single-crystal silicon, the fluorescence peaks of ruby, different Raman bands of pristine C_{60}, etc. In each case, excellent agreement was observed between our measurements and the well-known results for each one of these samples.[30–32,36–38] Since it is known that C_{60} can be polymerized under laser irradiation, Raman spectra were measured at selected pressures for different power levels of the argon ion laser between 20 and 100 mW. In the final analysis, care was taken to account for the laser power dependence of the spectra. Having loaded the sample and the pressure transmitting medium, four different sets of measurements were made by (i) increasing the pressure from almost ambient to 31.1 GPa, (ii) decreasing the pressure from 31.1 GPa down to almost ambient, (iii) once again increasing the pressure from almost ambient to 27 GPa, and finally (iv) releasing the pressure down to ambient, after which the sample was recovered for x-ray diffraction (XRD) analysis (labeled as the ''recovered sample'' in the remainder of the text). In the following, these pressure sequences are labeled, for the sake of clarity, as the first, second, third, and fourth pressure sequences.

The x-ray diffraction (XRD) measurements were made by using a Rigaku/Curved IP two-dimensional x-ray diffractometer system. This diffractometer uses a well-collimated (diameter about 300 μm) x-ray beam of wavelength $=0.228\,97$ nm from a Cr target (K_α line) and a cylindrical imaging plate. The system can measure 2D x-ray diffraction image over a broad range, covering 204° 2θ horizontally and $\pm45°$ 2θ vertically from the direct beam position. In transmission, the complete area is recorded simultaneously (complete Debye Sherrer rings) with $2\theta<45°$. Integrating out the χ dimension of the recorded 2D image produces intensity vs 2θ plot, the conventional powder pattern, which can be analyzed by using the powder-diffraction analysis software for identifying the structure of the material, etc.[39]

III. RESULTS AND DISCUSSION

A. Raman spectroscopy

Representative Raman spectra in the vicinity of the $H_g(7)$, $A_g(2)$, and $H_g(8)$ modes, as well as a 1625-cm^{-1} band of C_{60} measured at different pressures up to 31.1 GPa at room temperature, are shown in Fig. 1(a). A reference spec-

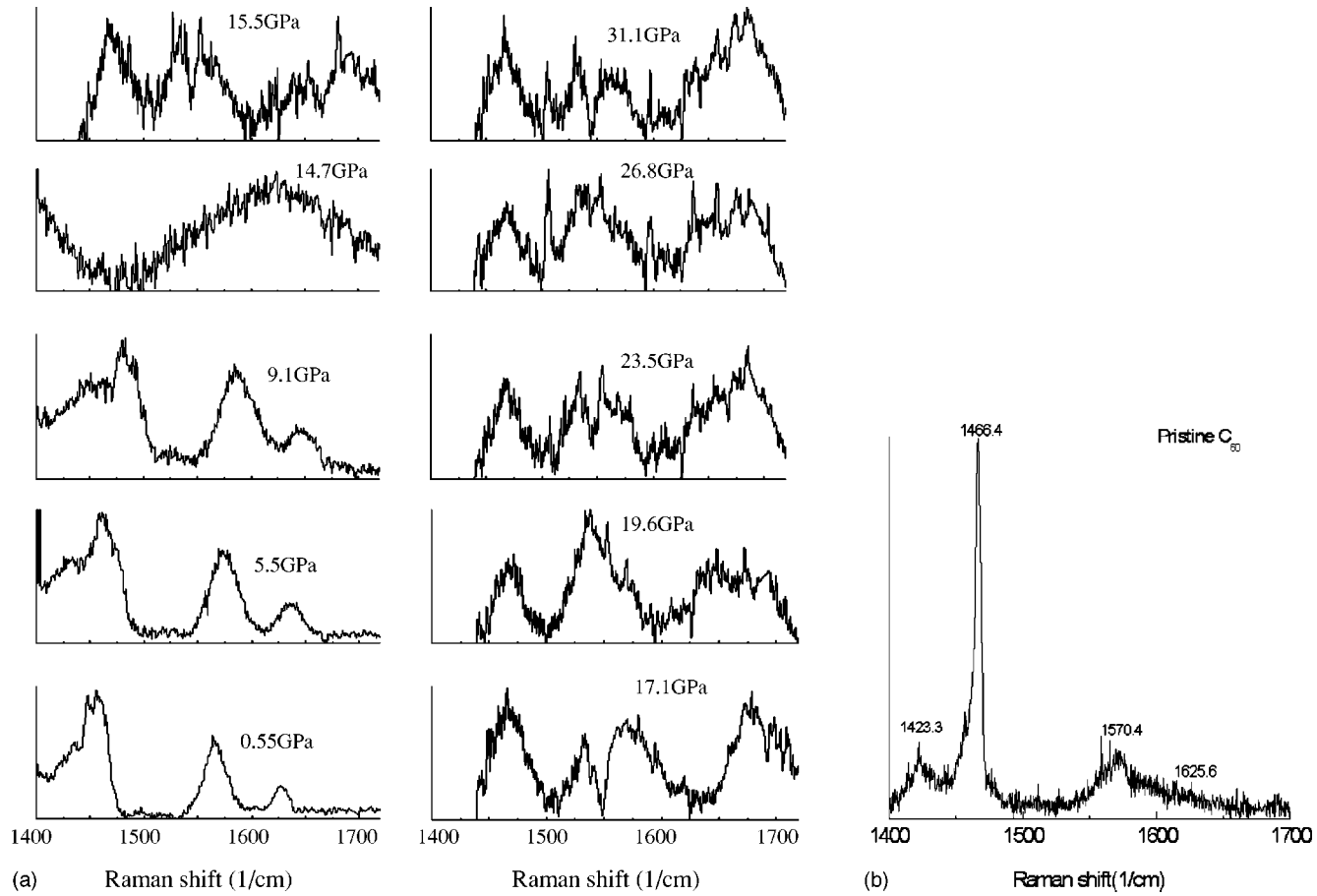

FIG. 1. (a) Raman spectra measured for nonhydrostatic conditions for C_{60} powder compressed in a diamond anvil cell under different pressures, in the range from 0.55 to 31.1 GPa, at room temperature. (b) Raman spectra measured for pristine C_{60} powder under ambient conditions.

trum measured for pristine C_{60} under ambient conditions is also shown in Fig. 1(b). The reference spectrum, clearly showing $H_g(7)$, $A_g(2)$, and $H_g(8)$ bands with Raman shifts of 1423, 1466, and 1570 cm^{-1}, respectively, is in excellent agreement with the well-known Raman spectrum characteristic of pristine C_{60}.[40,41] In agreement with published results,[17] the Raman bands of compressed C_{60} are weak in comparison to the shape of these bands measured under ambient conditions, particularly the $A_g(2)$ mode. There are two reasons for the weakness of the Raman signal; namely, a relatively small cross sections for the inelastic scattering of light and a very small amount of sample inside the 200-μm-diameter hole in $<$250-μm-thick gasket in the DAC. The mean frequencies of the Raman bands, identified with the $H_g(7)$, $A_g(2)$, $H_g(8)$ modes and the 1625-cm^{-1} band of C_{60} are plotted as a function of pressure in Fig. 2. The data on the most pronounced $A_g(2)$ band are collected from a large number of measurements that were made (i) by applying uniaxial as well as hydrostatic pressures (up to about 10 GPa) and (ii) by running the spectrometer at high and very high resolutions [FWHM$=(4.5\pm0.1)$ and (2.2 ± 0.1) cm^{-1} for the 1332 cm^{-1} diamond line, respectively]. The pressure dependence of the most pronounced $A_g(2)$ band is remarkable and it shows that (i) the use of the transmitting medium has little effect on the frequencies of the $A_g(2)$ Raman band up to about 4 GPa, (ii) however, for $4<P<13$ GPa, the transmitting medium affects the pressure dependence of the $A_g(2)$ band. In experiments conducted without the use of the transmitting medium, we observe clearly in the upper inset of Fig. 2 that (i) the frequency of the $A_g(2)$ band increases linearly with increasing pressure up to about 4 GPa, (ii) between about 4 and 8.28 GPa, these frequencies do not follow the linearity observed up to 4 GPa. Over this range of pressures, the measured frequencies are significantly lower than the values expected from an extrapolation of the low-pressure linear behavior. We observe a turnaround in the frequencies at around 7.26 GPa, above which they follow the linear pressure dependence observed from ambient to about 4 GPa. In the case of the data collected by using the pressure-transmitting medium, we observe that the frequency of the $A_g(2)$ band increases with increasing pressure from almost ambient to 5.38 GPa. Between 5.38 and 23.5 GPa, the measured frequencies deviate from this linear dependence. In this case, a turnaround in the values of the frequency is observed to occur at about 13.1 GPa. The pressure dependence of the $A_g(2)$ band is qualitatively similar in that the frequency of this band increases linearly with pressure from ambient to some pressure, deviates from this low-pressure linearity over a certain range of intermediate pressures, and returns to the low-pressure linear dependence at high pres-

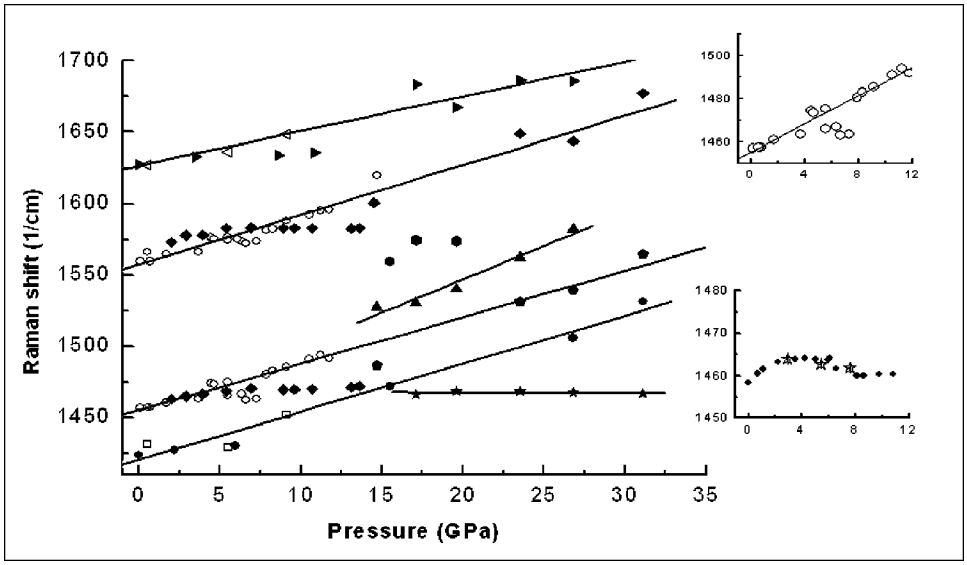

FIG. 2. Mean frequencies of the $H_g(7)$, $A_g(2)$, $H_g(8)$, and 1625-cm^{-1} Raman bands as a function of pressure, for the first pressure sequence (pressure increased from almost ambient to 31.1 GPa) at room temperature. The open (unfilled) symbols represent data obtained from Raman spectra measured without the use of a pressure transmitting medium in the DAC (uniaxial pressures). The lines are drawn only to aid the eyes. The structural phase transitions are evidenced by (i) deviations from a linear pressure dependence beginning at around 4 GPa, and (ii) appearance of additional bands at pressures higher than about 15 GPa. The upper inset shows details of the nonlinear behavior for the frequencies of the $A_g(2)$ band measured without the use of the pressure transmitting medium in the DAC. The lower inset shows evidence for reversible behavior of the pressure dependence of the spectra measured using the transmitting medium in the DAC (filled circles represent data for increasing pressures; and the stars represent data for decresing pressures).

sures. As the lower inset in Fig. 2 shows, the nonlinear pressure dependence of the $A_g(2)$ band for $0 \leqslant P \leqslant 8$ GPa is reversible. The deviations from the linear behavior observed at low pressures may signal the occurrence of a phase transition. While certain works report observations of structural phase transitions in the range 4–6 GPa, others report linear pressure dependence of the Raman shifts up to about 10 GPa. The occurrence of phase transitions at $P \leqslant 10$ GPa at room temperature is supported by several published works. One of the strongest evidences for a phase transition in pristine C_{60}, whereby its simple cubic structure changes into 1D orthorhombic polymerized phase, comes from the IR spectroscopy study by Yamawaki *et al.*,[16] who observed the appearance of different absorption bands and marked reduction in the intensity of the original bands at about 4 GPa due to pressure (hydrostatic) induced polymerization of C_{60}. Yoo and Nellis[17] also reported a phase transformation, albeit at a higher pressure, from weakly interacting C_{60} molecules to strongly interacting C_{60} agglomerates or networks. These authors observed that all of the vibrational modes shifted linearly with pressure up to about 10 GPa and deviated from linearity with the appearance of a ''knee'' between 10 and 15 GPa. Additionally, the volume compression data for C_{60} at room temperature[42,43] have shown evidence for a phase transition at $P \leqslant 6$ GPa. Under hydrostatic conditions, the volume was observed to decrease smoothly with increasing pressure up to about 22 GPa. However, under nonhydrostatic conditions, a much smaller compression of C_{60} observed above about 5 GPa is believed to be evidence for the room-temperature polymerization of C_{60}. Contrary to these results, which support a phase transition at around 4–6 GPa, some of the other studies observe an almost linear pressure dependence of the Raman shifts over the same range of pressures. Tolbert *et al.*[14] conducted Raman experiments on C_{60} crystals grown by heating the C_{60} powder in a temperature gradient under 10^{-6} Torr. They used either methanol:ethanol:water (16:3:1), or liquid nitrogen, or liquid argon for the pressure transmitting medium in the DAC and measured Raman spectra as functions of pressure up to 18 GPa and as functions of temperature between 4 and 360 K. Contrary to our findings, these authors observed neither significant changes due to the use of the pressure transmitting medium nor deviations from linearity up to about 10 GPa. On the other hand, Chandrabhas *et al.*[15] observed considerable softening of the $A_g(2)$ mode around 0.35 GPa. They observed significant increase in the linewidth and decrease in the intensity of the $A_g(2)$ mode with increasing pressures up to about 12.7 GPa. Although these authors did not particularly address the occurrence of a phase transition, their data clearly indicate a change in the pressure dependence of the frequency of the $A_g(2)$ mode around 3 GPa. Whether this change in the slope of the Raman frequencies vs pressure corresponds to a phase transition (similar to the pressure-induced phase transition to the rotation-free simple cubic phase at about 2.5 GPa observed by Meletov *et al.*[2]) remains a possibility. Meletov *et al.* have studied the pressure dependence of the Raman spectra of C_{60} single crystals up to about 7.2 GPa at room temperature. They observed two phase transitions, one at 0.4 GPa and another at 2.5 GPa. These pressure-induced phase transitions were attributed to orientational ordering from fcc to sc structure, and a rotation-free orientationally ordered sc phase, respectively. Haines *et al.*[44]

have studied C_{60} up to 28 GPa by XRD and observed a significant broadening of the diffraction lines above 10 GPa and diffuse scattering at 23 GPa. They also observed a featureless pattern at 28 GPa due to the highly disorganized nature of the material at this pressure. Additional discussion of the similarities and differences between the experimental conditions in several of these works, and other possible reasons for the observed nonlinear pressure dependence of the Raman shifts in our data, will be reported elsewhere.[32]

In view of these results, the main features of the pressure dependence of the $A_g(2)$ band up to about 31.1 GPa can therefore be summarized as follows: (i) the frequency of the $A_g(2)$ band increases linearly with increasing uniaxial pressure between ambient and 4 GPa, (ii) between 4 and 8 GPa, these frequencies deviate from linearity, exhibit a turnaround at about 7.26 GPa, and then resume the linear pressure dependence up to 31.1 GPa, (iii) under hydrostatic conditions, the pressure dependence of the $A_g(2)$ band is qualitatively similar. Although the range of the linear behavior and the turnaround pressure are different, (iv) as is clear from Fig. 1(a), a major change in the shape of the Raman spectrum occurs at around 14.7 GPa. The spectrum at 14.7 GPa is exceedingly broad and it probably encompasses contributions from other neighboring bands, indicating the occurrence of a phase transition at about 14.7 GPa, and (v) yet another change in the shape of the spectrum occurs at around 27 GPa, where newer bands appear. These observations are in good agreement with previously published data on HPHT quenched samples[2] and they signal the occurrence of structural phase transitions in the material. In this context, it is important to note that Okada *et al.*,[24] based on their calculations using density-functional theory, had predicted a phase transformation of C_{60} from its 2D polymerized tetragonal phase to 3D polymerized structure under uniaxial pressure of about 20 GPa. It is interesting to note that similar changes are observed in HPHT quenched samples as well as in pristine C_{60} compressed in the present work.

In Fig. 3, we show the pressure dependence of the Raman frequencies for the second and third pressure sequences, which consisted of (i) pressure release; releasing pressure in small steps starting from 31.1 GPa down to almost ambient pressure, and (ii) once again increase of pressure from ambient to about 27.5 GPa. The frequencies of these Raman bands are more or less independent of pressure after the material had been compressed under 31.1 GPa. Figure 4 shows spectra recorded for the sample under 31.1 GPa as well as for the recovered sample. There is hardly any change in the $A_g(2)$ band observed in these two spectra. It is clear that the sample, having been compressed to 31.1 GPa at room temperature in the first pressure sequence, retains its high-pressure (31.1 GPa) phase, which can be characterized with Raman bands of frequencies of about 1468, 1538, and 1680 cm^{-1}. In the following, we take advantage of this finding and characterize the structure of the high-pressure (31.1 GPa) phase of the material by conducting x-ray diffraction analysis.

B. X-ray diffraction

Figure 5 shows XRD spectra measured by using above described 300-μm-diameter x-ray beam of wavelength

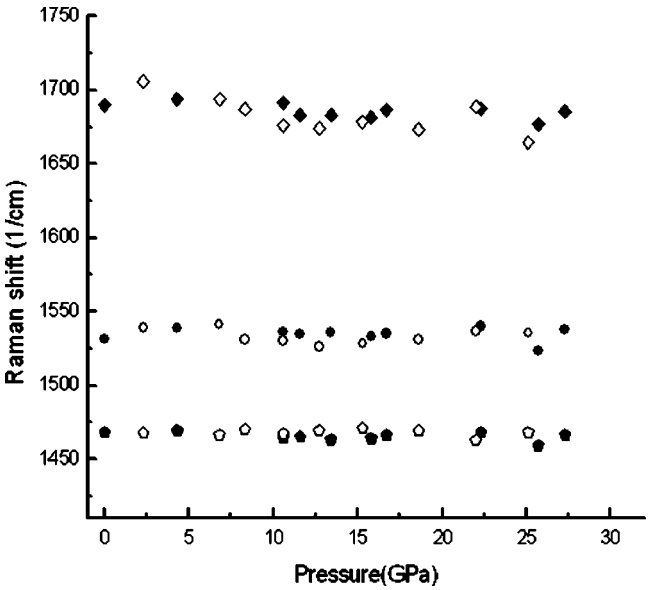

FIG. 3. Mean frequencies of the $H_g(7)$, $A_g(2)$, $H_g(8)$, and 1625-cm^{-1} Raman bands as a function of pressure, for the second pressure sequence (filled symbols, pressure released from 31.1 GPa to almost ambient) and third pressure sequence (open symbols, once again, pressure increased from almost ambient to 27.5 GPa) at room temperature. The sample was loaded with the transmitting medium in the DAC.

$= 0.228\,97$ nm from a Cr target (K_α line). These spectra were measured for the C_{60} sample recovered [Fig. 5(a)] after completion of all four pressure sequences described above and pristine C_{60} [Fig. 5(b)]. During these experiments, the sample had been subjected to the following sequence of increasing/decreasing pressure sequences: (i) ambient to 31.1 GPa, (ii) 31.1 GPa to ambient, (iii) ambient to 27.5 GPa, and finally (iv) pressure release down to ambient, after which the sample was recovered for XRD analysis. The Debye Scherrer rings, measured for the reference C_{60} powder and recovered sample, are also shown in Fig. 5. The rings are circular in shape with spots indicating preferential orientation of the grains. In the case of the recovered sample (31.1-GPa phase), the preferred orientation of the grains may be due to the fact that the pressure transmitting medium becomes nonhydrostatic above about 10 GPa. Consequently, the material must have been compressed uniaxialy above this pressure and certainly at around 31.1 GPa, the highest pressure applied in the present investigations. Additionally, as discussed under Experimental Details, it is possible that the sample had experienced shear deformation to some extent. In Table 1, we list details for a total of 13 peaks resolved in the XRD spectrum of the recovered sample. In addition to 2θ values (peak centroids), the table also includes results for interplanar spacing d_{hkl}, relative intensity, and FWHM of each peak resolved.[32]

In order to better understand the complex structure of the material, we have carried out simulations for the intensity vs 2θ patterns using crystallographic parameters for the expected phases of the material. The simulations of the x-ray patterns were made by starting with published values of the atomic coordinates for the body-centered orthorhombic

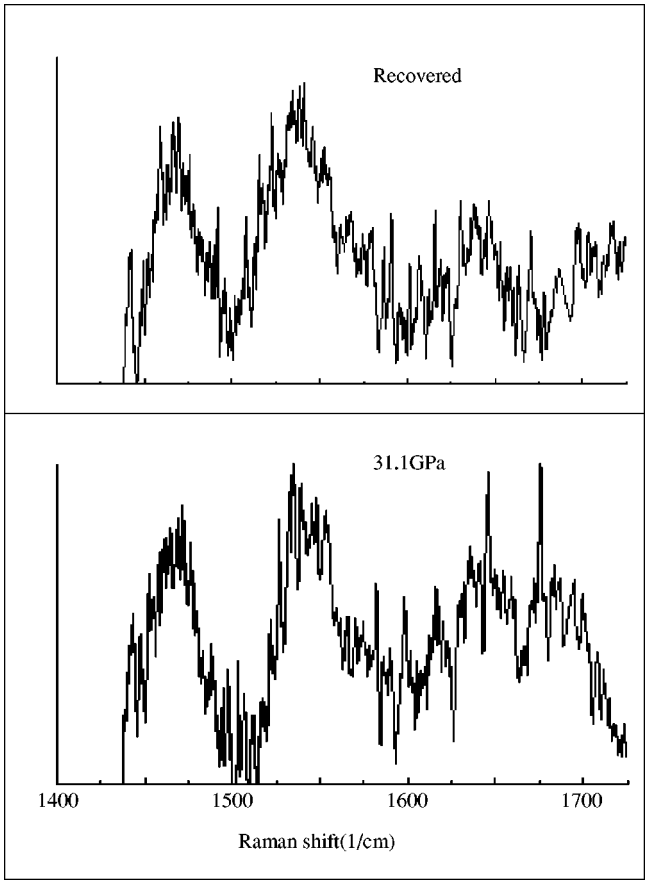

FIG. 4. Raman spectra measured for C_{60} compressed under 31.1 GPa and recovered sample. As described in the text, these data were obtained by loading the sample with the transmitting medium in the DAC.

(BCO, *Immm*), rhombohedral ($R\bar{3}m$), hard and superhard body-centered cubic, and tetragonal structures.[24,26,27,45–47] We made refinements in these simulations by varying, within reasonable limits, the crystallographic parameters (lattice constants were varied up to $\pm 2\%$ from their values given in these references) in order to improve agreement between the measured spectra and the simulations. In these exercises, if the centroids of the simulated and measured peaks (2θ values) were within $\pm 0.1°$, the simulation was considered to be in agreement with the measurement. As the results listed in the table show, the recovered material consists of a mixture of the body-centered orthorhombic (*Immm*, 38%), rhombohedral ($R\bar{3}m$, 30%), and an unidentified structure. The crystallographic parameters for the BCO (*Immm*) and *R* ($R\bar{3}m$) phases, that provide the best fit for the measured XRD spectrum, are $a=0.911$ nm, $b=0.978$ nm, $c=1.450$ nm, and $r_{av}=0.355$ nm for the BCO (*Immm*), and $a=0.916$ nm, $c=2.450$ nm, and $r_{av}=0.36$ nm for the $R\bar{3}m$ phases, respectively. These parameters are in excellent agreement with those published previously.[46] Although the remaining 32% of the mixture is not clearly identified as yet, we have ruled out the presence of so-called hard and superhard phases in the recovered material. At variance with results on HPHT quenched samples,[27,47] we do not obtain good fits between

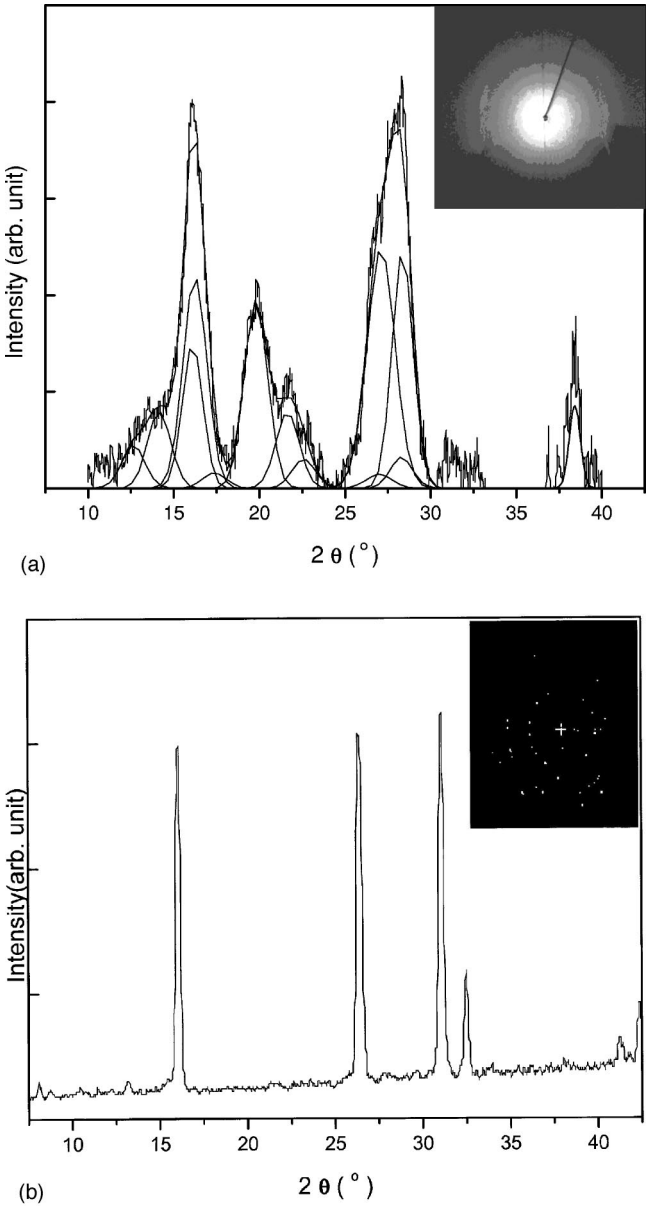

FIG. 5. (a) XRD spectra measured for the high-pressure (31.1 GPa) phase recovered after completion of all four pressure sequences between ambient and 31.1 GPa described in the text. The sample was loaded in the DAC along with the transmitting medium. The insets show Debye Sherrer rings. (b) XRD spectra measured for pristine C_{60} powder. The insets show Debye Sherrer rings. The results of the curve fit, representing the structures listed in Table 1, are also shown.

the measured and simulated spectra when simulations are made by using crystallographic parameters for the hard and superhard structures. These hard and superhard structures have been identified previously in the HPHT quenched samples that were obtained after 13 GPa at 670 and 820 K, respectively. The unit-cell parameters for these structures have been determined in earlier publications as $a=0.873$ nm, $b=0.916$ nm, $c=1.294$ nm, and $V=0.517$ nm^3, for the hard structure, and $a=0.867$ nm, $b=0.881$ nm, $c=1.260$ nm, and $V=0.481$ nm^3, for the super-

TABLE I. XRD analysis of the recovered material (31.1-GPa phase). The sample was loaded with the transmitting medium in the DAC and subjected to the pressure sequences described in the text.

Peak Number	2θ	(hkl)	d_{hkl} (Å)	Relative intensity (%)	FWHM	Identified structure
1	12.642			14.8	1.36	
2	14.146			26.4	1.36	
3	16.097	003	8.167	43.6	1.19	rhombohedral
4	16.233	011	8.108	74.7	1.39	BCO
5	17.369	101	7.547	5.3	1.36	rhombohedral
6	19.798	102	6.659	64.6	1.36	rhombohedral
7	21.634	004	6.125	26.3	1.36	rhombohedral
8	22.584			10.0	1.36	
9	26.986	112	4.907	5.3	1.49	BCO
10	27.096	020	4.890	100.00	1.64	BCO
11	28.287			10.2	1.30	
12	28.355			73.7	1.22	
13	38.410			12.3	0.74	

hard structure.[27] Additional work is in progress to determine details of the structural and electronic properties of similar C_{60} based materials.[48]

In spite of significant research, the structure of C_{60} subjected to high pressures, $P \geqslant 30$ GPa at room temperature, is not yet clearly understood. We present a brief discussion of some of the recent and relevant data and re-emphasize important differences between the experimental conditions of our and previous experiments. Hopefully, this will help in arriving at a better understanding of our results and stimulate further investigations of the structure and properties of non-HPHT C_{60} compressed under high pressures at room temperature. A meaningful comparison between the present results and the results of the previous experiments should be done in the context of the experimental conditions, namely, (i) the range and nature of applied pressures (hydrostatic, nonhydrostatic, and shear deformation), (ii) sample temperature, (iii) irradiation conditions, i.e., laser power, spectral details, duration of irradiation, etc. Although several previous studies have presented evidence for amorphous structure of compressed C_{60}, our data show that the recovered material (31.1-GPa phase) consists of body-centered orthorhombic, rhombohedral, and an unidentified structure. In the following, we present a brief discussion of relevant published results, some of which support our findings in that crystalline structures are present in the compressed material. Duclos *et al.*[42] have studied compression of C_{60} under both hydrostatic and nonhydrostatic conditions. They observed that the fcc structure remains stable under hydrostatic conditions up to about 20 GPa and a transition to a crystallographic structure of lower symmetry occurs at about 16 GPa. Nunez-Regueiro *et al.*[49] have presented evidence for the existence of polycrystalline diamond and preponderantly tetrahedrically coordinated amorphous carbon phase in C_{60} that was compressed by applying nonhydrostatic pressures of about 20 GPa. Iwasa *et al.*[45] observed two different polymeric phases in C_{60} heated under 5 GPa. At low temperatures (573–673 K) and 5 GPa, they observed a disordered phase, believed to be fcc with some distortion of the unit cell (so-called ''soft fcc''). When treated at 773–1073 K at 5 GPa, a rhombohedral structure was observed. Oszlanyi *et al.*[50] have observed an amorphous phase of C_{60} compressed to about 10 GPa. Snoke *et al.*[51] also observed fullerene Raman peaks up to about 20 GPa. At around 22 GPa the two strongest high-frequency peaks were observed to merge into one band, which persisted up to about 42 GPa with irreversible Raman spectrum upon pressure release down to ambient pressure. On the basis of the Raman spectra of various carbon forms, Snoke *et al.* identified the high-pressure phase to be amorphous carbon. Moshary *et al.*[52] studied the shift of the optical edge as a function of pressure up to about 35 GPa and observed an irreversible transition to a ''transparent phase'' between 17 and 25 GPa. Based on the Raman spectrum of the depressurized sample, they concluded that C_{60} was destroyed at the high-pressure transition producing a ''collapsed fullerite'' (CF) phase, which they believed to be a new amorphous carbon. The XRD measurements of Haines and Leger[44] confirmed the formation of the CF phase above 23 GPa and observed featureless XRD data at 28 GPa indicating transformation to amorphous carbon. Blank *et al.*[19] have carried out a detailed study of the structure of C_{60} fullerite up to about 37 GPa with shear deformation. They found two states of fullerite at high pressures under controlled shear deformation, which persisted after pressure release. Blank *et al.* further observed, from Raman spectroscopy measurements, that C_{60} molecules persisted in both states with evidence for pressure-induced polymerization. These authors presented evidence for phase transitions at 0.3, 2.3, 6, and 18 GPa. At 2.3 GPa, the sample became opaque in the visible, but remained transparent in the IR. At the transition at 6 GPa, the sample became opaque in both visible and near IR regions. The transition at 18 GPa recovers sample transparency in the visible and near IR regions. A state produced at $P > 18$ GPa with shear deformation was observed to be harder than diamond and transparent in the near infrared and visible regions. Blank *et al.* assumed that C_{60} molecules were preserved in fullerite in both of these high-pressure states, their structures being distinguishable by the degree of polymerization. Besides confirming the prediction by Ruoff and Ruoff[53] that at high pressures, when the intermolecular distances in fullerite become comparable to the intramolecular C–C bonds, fullerites may be harder than diamond, the study by Blank *et al.* reaffirmed the fact that different geometrical parameters cause different values of the pressure gradients and different conditions of deformation. All of this affects the phase transformation process and relative proportions of different phases in the sample. Meletov *et al.*[54] have studied structural stability of the rhombohedral 2D polymeric phase of C_{60} in HPHT samples by using Raman spectroscopy. The XRD analysis of the starting HPHT sample showed that the crystal structure of the polymer was rhombohedral ($R\bar{3}m$, with $a = 0.922$ nm and $c = 2.46$ nm). They observed significant changes in the Raman spectrum at $P \sim 15$ GPa, where the spectrum became very diffuse and lost its fine structure. They further observed that at $P > 15$ GPa, Raman spectra changed drastically from the initial spectrum of the 2D

rhombohedral phase. These authors concluded that the 2D rhombohedral polymeric phase undergoes an irreversible change to a disordered phase at $P>15$ GPa, and noted that this observation was not in step with the theoretical calculations by Burgos *et al.*,[26] which predicted regular covalent bonding between the polymeric sheets under pressure. Agafonov *et al.*[55] have observed that a pressure-temperature treatment of C_{60} at 1.5 GPa and 723 K produces an orthorhombic structure O', which is significantly different from the orthorhombic phase formed at 8 GPa and 573 K. The unit-cell volume of the O' phase is larger than that of the O phase; 0.658 nm^3 vs 0.641–0.650 nm^3 for the O phase. These authors provide the unit-cell parameters for this new O' phase as $a=(0.9098\pm0.0006)$ nm, $b=(0.983\pm0.001)$ nm, $c=(1.472\pm0.002)$ nm, which should be compared with the unit-cell parameters for the O phase, $a=(0.926-0.929)$ nm, $b=(0.981-0.988)$ nm, $c=(1.408-1.422)$ nm. Based on the Raman, XRD, and electron-diffraction analyses, these authors conclude, in agreement with earlier observation by Marques *et al.*,[28] that this new phase (O') is a distorted fcc phase, and it is an intermediate stage for the tetragonal phase preferentially formed at higher pressure-temperature conditions.

It is clear from the above discussion that phase transformations of C_{60} under high pressure (hydrostatic, nonhydrostatic, shear deformations) and high temperature are complex and not completely understood. The high-pressure (31.1 GPa) structure observed in our sample, i.e., a mixture of the body-centered orthorhombic, rhombohedral, and an unidentified phase, is different in that we do not observe an amorphous phase in the material. The cell parameters obtained from our XRD analysis, $a=0.911$ nm, $b=0.978$ nm, $c=1.450$ nm, and $r_{av}=0.355$ nm for the BCO (*Immm*), and $a=0.916$ nm, $c=2.450$ nm, and $r_{av}=0.36$ nm for the $R\bar{3}m$ phases, respectively, are in excellent agreement with known results.[46] Additionally, a recent study[56] shows that HPHT treatment of C_{60} (6 GPa at 1025–1050 K) can produce magnetically ordered rhombohedral C_{60} with cell parameters $a=0.9204$ nm and $b=2.461$ nm, which are in excellent agreement with our results for the rhombohedral phase. Although we are not certain about the precise reasons for the absence of an amorphous phase in our sample, we draw attention to the following experimental conditions, which might play a role in the final structure of the material, (i) our pristine C_{60} sample had been subjected to aforementioned four pressure sequences prior to recovery for the XRD analysis, (ii) the material was compressed under nonhydrostatic conditions above about 10 GPa, where the pressure transmitting medium no longer offers hydrostatic conditions, (iii) it is possible that the material experiences shear deformations, (iv) the material was exposed to argon-ion laser irradiation for extended periods (several hours/day on and off for several weeks) during our experiments, and (v) the pressure transmitting medium may have influenced in some hitherto unknown manner the structure of the recovered material. The precise reasons for the observed structure are uncertain at this time. What is certain is the fact that the material can be polymerized by either laser irradiation, or by application of high pressures, or by a combination of these variables. As it is noted by Sundqvist,[22] random lengths and directions of linearly polymerized molecules create disorder in the structure of the material. Disorder is not unexpected, since polymerization is almost always carried out by heating a sample in the fcc phase, with almost freely rotating molecules and thus no preferred bonding directions. Additionally, the pressure gradients on the sample could promote disorder. Although the pressure-treated materials are usually disordered, it has also been reported[57] that large single crystals could also be polymerized into well ordered states by application of hydrostatic pressures 1.1 GPa at 550–585 K. Much additional research is needed to better understand the rich and complex phase diagram of C_{60}, especially when the material is subjected to extended laser irradiation under high pressures (inclusive of hydrostatic, nonhydrostatic, and shear deformation) at room temperature as well as at elevated temperatures. Additional research is also needed to better understand the nature of the nonlinear pressure dependence of the $A_g(2)$ band of C_{60} between 4 and 7 GPa (uniaxial pressures) as well as the role of the pressure-transmitting medium in the observed pressure dependencies.

IV. CONCLUSIONS

In conclusion, we have measured Raman spectra for pristine C_{60} compressed in diamond anvil cell for a range of pressures from almost ambient to 31.1 GPa at room temperature. We have conducted a series of experiments with and without the use of a pressure transmitting medium in the DAC. In agreement with previously published Raman spectroscopy data, we observe changes in the pressure dependence of certain Raman modes that are consistent with the occurrence of several structural phase transitions of C_{60} under high pressures at room temperature. Upon lowering the pressure from 31.1 GPa down to almost ambient, the details of the Raman bands remain more or less unchanged. The material therefore retains its structure that it had acquired at high pressures up to 31.1 GPa. XRD measurements on the recovered material (high-pressure phase) by using a 300-μm-diameter collimated beam show that the high-pressure phase consists of a mixture of the BCO (*Immm*), rhombohedral ($R\bar{3}m$), and an unidentified structure. The cell parameters for the identified phases are in excellent agreement with the published results. The Debye Scherrer rings for the recovered sample are observed to be circular in shape with spots indicating preferential orientation of the grains in the high-pressure phase of the material.

ACKNOWLEDGMENTS

One of the authors (S.C.S.) is grateful to Dr. R. Hemley, Dr. A. F. Goncharov, and Dr. D. Sciferl for sharing the ''tricks-of-the-trade'' of high-pressure research with a diamond anvil cell. This research was supported, in part, by grants from the Department of Energy (Grant No. DE-FG0300ER45840) and the Welch Foundation, Houston, Grant No. Y-1484.

*Corresponding author. Email address: sharma@uta.edu

[1] A. V. Talyzin, L. S. Dubrovinsky, T. Le Bihan, and U. Jansson, Phys. Rev. B **65**, 245413 (2002).

[2] K. P. Meletov, J. Arvanitidis, E. Tsilika, S. Assimopoulos, G. A. Kourouklis, S. Ves, A. Soldatov, and K. Prassides, Phys. Rev. B **63**, 054106 (2001).

[3] B. Sundqvist, Phys. Status Solidi B **223**, 469 (2001).

[4] V. A. Davydov, L. S. Kashevarova, A. V. Rakhmanina, V. M. Senyavin, R. Ceolin, H. Szwarc, H. Allouchi, and V. Agafonov, Phys. Rev. B **61**, 11 936 (2000).

[5] L. Forro and L. Mihaly, Rep. Prog. Phys. **64**, 649 (2001).

[6] *Fullerene Polymers and Fullerene Polymer Composites*, edited by P. C. Eklund and A. M. Rao (Springer-Verlag, Berlin, 1999).

[7] V. A. Davydov, L. S. Kashevarova, A. V. Rakhmanina, V. M. Senyavin, O. P. Pronina, N. N. Oleynikoy, V. Agafonov, R. Ceolin, H. Allouchi, and H. Szwarc, Chem. Phys. Lett. **333**, 224 (2001).

[8] L. A. Chernozatonskii, N. R. Serebryanaya, and B. N. Mavrin, Chem. Phys. Lett. **316**, 199 (2000).

[9] V. A. Davydov, V. Agafonov, H. Allouchi, R. Ceolin, A. V. Dzyabchenko, and H. Szwarc, Synth. Met. **103**, 2415 (1999).

[10] M. E. Kozlov, M. Tokumoto, and K. Yakushi, Synth. Met. **86**, 2349 (1997).

[11] A. M. Rao, P. C. Eklund, J.-L. Hodeau, L. Marques, and M. Nunez-Regueiro, Phys. Rev. B **55**, 4766 (1997).

[12] V. V. Brazhkin, A. G. Lyapin, and S. V. Popova, JETP Lett. **64**, 802 (1996) [Pis'ma Zh. Eksp. Teor. Fiz. **64**, 755 (1996)].

[13] G. Oszlanyi and L. Forro, Solid State Commun. **93**, 265 (1995).

[14] S. H. Tolbert, A. P. Alivisatos, H. E. Lorenzana, M. B. Kruger, and R. Jeanloz, Chem. Phys. Lett. **188**, 163 (1992).

[15] N. Chandrabhas, M. N. Shashikala, D. V. S. Muthu, A. K. Sood, and C. N. R. Rao, Chem. Phys. Lett. **197**, 319 (1992).

[16] H. Yamawaki, M. Yoshida, Y. Kakudate, S. Usuba, H. Yokoi, S. Fujiwara, K. Aoki, R. Ruoff, R. Malhotra, and D. Lorents, J. Phys. Chem. **97**, 11 161 (1993).

[17] C. S. Yoo and W. J. Nellis, Chem. Phys. Lett. **198**, 379 (1992).

[18] K. Nishikawa and Y. Miyamoto, J. Phys. Chem. Solids **56**, 577 (1995).

[19] V. Blank, M. Popov, S. Buga, V. Davydov, V. N. Denisov, A. N. Ivlev, B. N. Mavrin, V. Agafonov, R. Ceolin, H. Szwarc, and A. Rassat, Phys. Lett. A **188**, 281 (1994).

[20] M. S. Dresselhaus, G. Dresselhaus, and P. C. Eklund, *Science of Fullerenes and Carbon Nanotubes* (Academic Press, New York, 1995).

[21] *Fullerenes*, edited by K. M. Kadish and R. S. Ruoff (Wiley Interscience, New York, 2000).

[22] B. Sundqvist, Adv. Phys. **48**, 1 (1999).

[23] V. A. Davydov, L. S. Kashevarova, A. V. Rakhmanina, V. Agafonov, H. Allouchi, R. Ceolin, A. V. Dzyabchenko, V. M. Senyavin, and H. Szwarc, Phys. Rev. B **58**, 14 786 (1998).

[24] S. Okada, S. Saito, and A. Oshiyama, Phys. Rev. Lett. **83**, 1986 (1999).

[25] G. B. Adams and J. B. Page, Phys. Status Solidi B **226**, 95 (2001).

[26] E. Burgos, E. Halac, R. Weht, H. Bonadeo, E. Artacho, and P. Ordejon, Phys. Rev. Lett. **85**, 2328 (2000).

[27] L. A. Chernozatonskii, N. R. Serebryanaya, and B. N. Mavrin, Chem. Phys. Lett. **316**, 199 (2000).

[28] L. Marques, J.-L. Hodeau, M. Nunez. Regueiro, and M. Perroux, Phys. Rev. B **54**, R12 633 (1996).

[29] V. D. Blank, V. N. Denisov, A. N. Ivlev, B. N. Mavrin, N. R. Serebryanaya, G. A. Dubitsky, S. N. Sulyanov, M. Yu. Popov, N. A. Lvova, S. G. Buga, and G. N. Kremkova, Carbon **36**, 1263 (1998).

[30] S. C. Sharma, B. Ha, J. H. Rhee, and Y. Li, in *Frontiers of High Pressure Research II: Applications of High Pressure to Low-Dimensional Novel Electronic Materials*, edited by H. D. Hochheimer, B. Kuchta, P. K. Dorhout, and J. L. Yarger, NATO Science Series Vol. 48 (Kluwer Academic Publishers, Dordrecht/Boston/London, 2001), p. 493.

[31] S. C. Sharma, B. Ha, J. H. Rhee, Y. Li, D. Singh, and R. Govinthasamy, in *Thin Films: Stresses and Mechanical Properties IX*, edited by C. S. Ozkan *et al.*, Mater. Res. Soc. Symp. Proc. No. **695** (Materials Research Society, Warrendale, PA, 2002), p. 97.

[32] D. Singh, Y. Li, and S. C. Sharma (unpublished); J. H. Rhee, D. Singh, Y. Li, and S. C. Sharma, Solid State Commun. **127**, 295 (2003).

[33] MER Corporation, Tucson, Arizona.

[34] R. M. Hazen and L. W. Finger, *Comparative Crystal Chemistry* (John Wiley & Sons, New York, 1982).

[35] A. Jayaraman, Rev. Mod. Phys. **55**, 65 (1983).

[36] S. C. Sharma, M. Green, R. C. Hyer, C. A. Dark, T. D. Black, A. R. Chourasia, D. R. Chopra, and K. K. Mishra, J. Mater. Res. **5**, 2424 (1990).

[37] R. C. Hyer, M. Green, and S. C. Sharma, Phys. Rev. B **49**, 14 573 (1994).

[38] M. Green, Ph.D. dissertation, University of Texas at Arlington, 1991.

[39] *Fast X-ray Diffractometer with Area Detector,* The Rigaku Journal **16**, 51 (1999).

[40] Z. H. Dong, P. Zhou, J. M. Holden, P. C. Eklund, M. S. Dresselhaus, and G. Dresselhaus, Phys. Rev. B **48**, 2862 (1993).

[41] J. L. Feldman, J. Q. Broughton, L. L. Boyer, D. E. Reich, and M. D. Kluger, Phys. Rev. B **46**, 12 731 (1992).

[42] S. J. Duclos, K. Brister, R. C. Haddon, A. R. Kortan, and F. A. Thiel, Nature (London) **351**, 380 (1991).

[43] H. A. Ludwig, W. H. Feitz, F. W. Hornung, K. Grube, B. Wagner, and G. J. Burkhart, Z. Phys. B: Condens. Matter **96**, 179 (1994).

[44] J. Haines and J. M. Leger, Solid State Commun. **90**, 361 (1994).

[45] Y. Iwasa, T. Arima, R. M. Fleming, T. Siegrist, O. Zhou, R. C. Haddon, L. J. Rothberg, K. B. Lyons, H. L. Carter, Jr., A. F. Hebard, R. Tycko, G. Dabbagh, J. J. Krajewski, G. A. Thomas, and T. Yagi, Science **264**, 1570 (1994).

[46] M. Nunez Regueiro, L. Marques, J. L. Hodeau, O. Béthoux, and M. Perroux, Phys. Rev. Lett. **74**, 278 (1995); V. A. Davydov, L. S. Kashevarova, A. V. Rakhmanina, V. Agafonov, R. Ceolin, and H. Szwarc, Carbon **35**, 735 (1997).

[47] V. D. Blank, S. G. Buga, N. R. Serebryanaya, V. N. Denisov, G. A. Dubitsky, A. N. Ivlev, B. N. Mavrin, and M. Y. Popov, Phys. Lett. A **205**, 208 (1995).

[48] B. Ha, J. H. Rhee, Y. Li, D. Singh, and S. C. Sharma, Surf. Sci. **520**, 186 (2002).

[49] M. Nunez-Regueiro, L. Abello, G. Lucazeau, and J.-L. Hodeau, Phys. Rev. B **46**, 9903 (1992).

[50] G. Oszlanyi, D. R. Allan, R. J. Cernik, G. Bushnell-Wye, G. Faigel, S. Pekker, and M. Tegze, Solid State Commun. **84**, 1081 (1992).

[51] D. W. Snoke, Y. S. Raptis, and K. Syassen, Phys. Rev. B **45**, 14 419 (1992).
[52] F. Moshary, N. H. Chen, I. F. Silvera, C. A. Brown, H. R. Dorn, M. S. de Vries, and D. S. Bethune, Phys. Rev. Lett. **69**, 466 (1992).
[53] R. S. Ruoff and A. L. Ruoff, Nature (London) **350**, 663 (1991).
[54] K. P. Meletov, J. Arvanitidis, G. A. Kourouklis, K. Prassides, and Y. Iwasa, Chem. Phys. Lett. **357**, 307 (2002).
[55] V. Agafonov, V. A. Davydov, L. S. Kashevarova, A. V. Rakhmanina, A. Kahn-Harari, P. Dubois, R. Ceolin, and H. Szwarc, Chem. Phys. Lett. **267**, 193 (1997).
[56] T. L. Makarova, B. Sundqvist, R. Hohne, P. Esquinazi, Y. Kopelevich, P. Scharff, V. A. Davydov, L. S. Kashevarova, and A. V. Rakhmanina, Nature (London) **413**, 716 (2001).
[57] R. Moret, P. Launois, P.-A. Persson, and B. Sundqvist, Europhys. Lett. **40**, 55 (1997).